BIOCHEMISTRY
including biophysical chemistry & molecular biology

Article

pubs.acs.org/biochemistry

Lengthening the Intersubunit Linker of Procaspase 3 Leads to Constitutive Activation

Sarah H. MacKenzie,[†] Joshua L. Schipper,[†] Erika J. England,[†] Melvin E. Thomas, III,[†] Kevin Blackburn,[†] Paul Swartz,[†] and A. Clay Clark*[,†,‡]

[†]Department of Molecular and Structural Biochemistry and [‡]Center for Comparative Medicine and Translational Research, North Carolina State University, Raleigh, North Carolina 27695, United States

Supporting Information

ABSTRACT: The conformational ensemble of procaspase 3, the primary executioner in apoptosis, contains two major forms, inactive and active, with the inactive state favored in the native ensemble. A region of the protein known as the intersubunit linker (IL) is cleaved during maturation, resulting in movement of the IL out of the dimer interface and subsequent active site formation (activation-by-cleavage mechanism). We examined two models for the role of the IL in maintaining the inactive conformer, an IL-extension model versus a hydrophobic cluster model, and we show that increasing the length of the IL by introducing 3−5 alanines results in constitutively active procaspases. Active site labeling and subsequent analyses by mass spectrometry show that the full-length zymogen is enzymatically active. We also show that minor populations of alternately cleaved procaspase result from processing at D169 when the normal cleavage site, D175, is unavailable. Importantly, the alternately cleaved proteins have little to no activity, but increased flexibility of the linker increases the exposure of D169. The data show that releasing the strain of the short IL, in and of itself, is not sufficient to populate the active conformer of the native ensemble. The IL must also allow for interactions that stabilize the active site, possibly from a combination of optimal length, flexibility in the IL, and specific contacts between the IL and interface. The results provide further evidence that substantial energy is required to shift the protein to the active conformer. As a result, the activation-by-cleavage mechanism dominates in the cell.

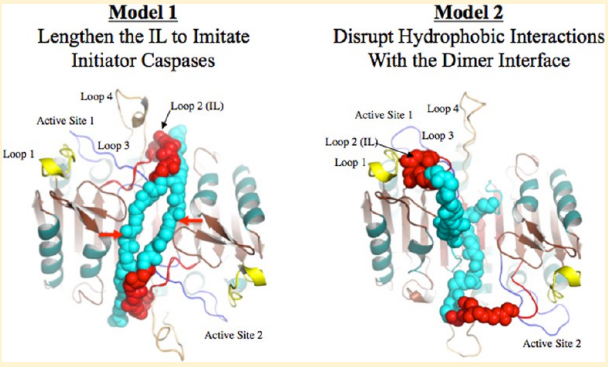

Caspases are a family of proteolytic enzymes that play a critical role in programmed cell death, or apoptosis. Defects in the regulatory mechanisms that control caspase activation have been observed in numerous diseases, ranging from neurodegenerative disorders such as Alzheimer's disease, in cases of too much cell death, to cancer, where cells may have reduced ability to carry out caspase-mediated apoptosis.[1] Apoptotic caspases are divided into two main groups: the initiators, which are initially activated through either intrinsic or extrinsic cell death signals, and the effectors, which are activated by the initiator caspases and are ultimately responsible for dismantling the cell. Caspase 3 is the key effector caspase, and its activation is the commitment step for apoptosis. These enzymes are initially expressed as inactive zymogens (procaspases) containing an N-terminal prodomain followed by large and small subunits that are connected by an intersubunit linker (IL). The zymogens form dimers, and during the process of activation the IL is proteolyzed at one or more sites and the prodomain is removed.[2] Although largely similar in structure, an important difference exists in the mechanism for enzyme activation between the initiator and effector caspases. In the case of initiator caspases (namely, caspases 8, 9, and 10), the zymogen exists as a stable monomer, and upstream cell death signals lead to its localization to activation scaffolds. The increase in local concentration on the scaffold drives dimerization, where the initiator procaspase becomes enzymatically active.[3] It is believed that, for the initiator caspases, the proteolytic processing of the IL that follows dimerization acts mainly to stabilize the dimer. In contrast, the zymogens of effector caspases (caspases 3, 6, and 7) are stable dimers, although they exhibit very little enzymatic activity, and cleavage of the IL by the initiator caspases results in full enzyme activation. As a result of cleavage, the IL is released from the dimer interface (DI), which allows active site loop 3 to form the base of the substrate-binding pocket (Figure 1A). In caspase 3, the side-chain of R164, which is immediately adjacent to the catalytic cysteine, intercalates between P201 on loop 3 and Y197 in the DI; these interactions are required for formation of the active site and are unable to form in the inactive zymogen (for a more complete description, see refs 4−6). The regulation of apoptotic signals is understandably important to the survival of an organism, and the difference in activation mechanisms allows for both the prevention of accidental initiation of apoptosis and

Received: June 19, 2013
Revised: August 9, 2013
Published: August 13, 2013

   dx.doi.org/10.1021/bi400793s | *Biochemistry* 2013, 52, 6219−6231

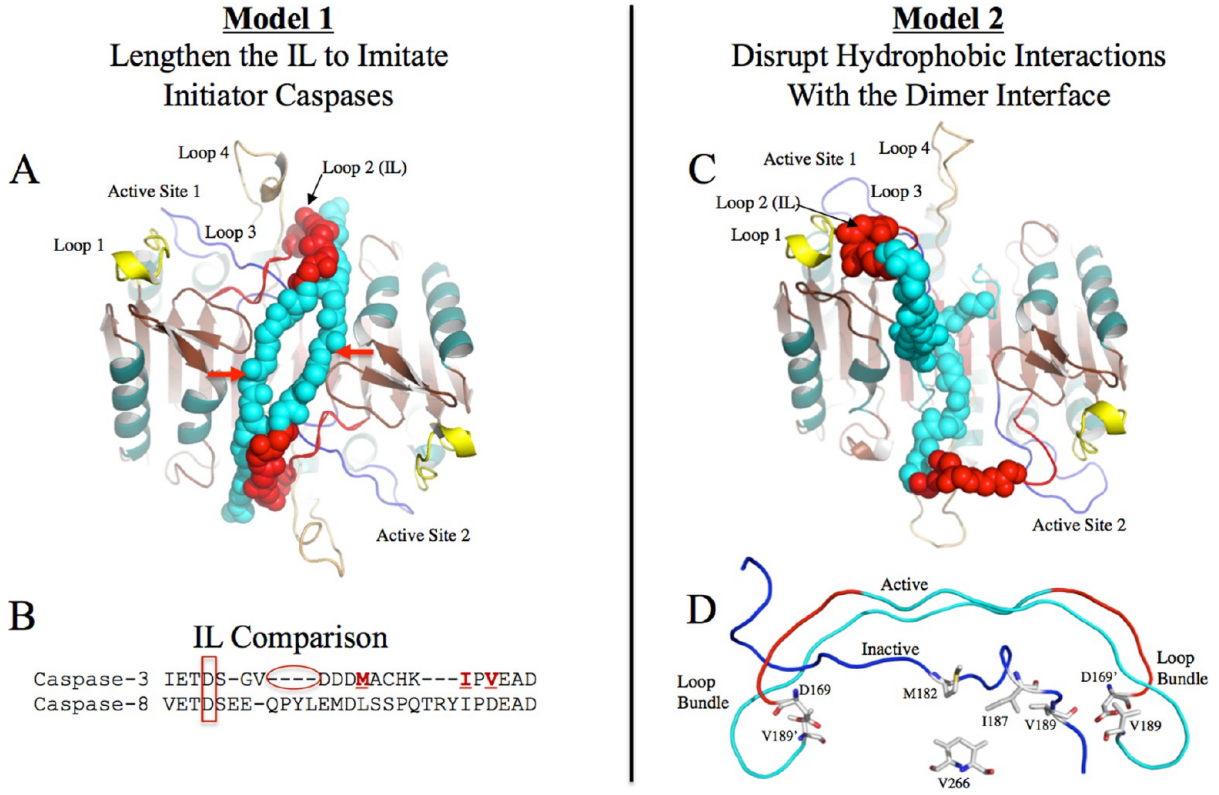

Figure 1. Proposed models for procaspase 3 activation. (A) Model of the active conformation of procaspase 3. Lengthening the intersubunit linker (IL) may allow the proenzyme to sample more conformations with a fully formed active site, mimicking initiator caspases (like caspase 8), which have longer ILs than the effector caspases. (B) Sequence alignment comparing a section of the IL of caspase 3 and caspase 8. The red box indicates the site of cleavage (D175 in caspase 3). Location of inserted residues is indicated by red arrows (panel A) or red oval (panel B), and hydrophobic amino acids discussed in the text are shown in red (see also panel D). (C) Model of the inactive conformation of procaspase 3. Hydrophobic residues in the IL may interact withV266 in the dimer interface, stabilizing the inactive conformation. For A and C, the backbone atoms of the IL are represented as spheres. (D) Comparison of position of the IL in the inactive or active conformation relative to the dimer interface (represented by V266). Hydrophobic groups in the IL (M182, I187, V189) are predicted to interact with V266. Loop bundle contacts between D169 and V189′ (from the second monomer) occur only in the active conformation. In panels A, C, and D, the cleavage site (D175) is represented by the change in color from red to cyan.

the ability to initiate a very robust apoptotic cascade when needed.

As caspases are increasingly targeted for the treatment of disease, a better understanding of procaspase conformational equilibria is important, in particular, why IL cleavage is required to fully activate the effector procaspases but not the initiators. In the strategy of activating caspase 3 to induce apoptosis in cancer cells,[5,7−9] current methods are greatly limited by the fact that these cells often overexpress caspase inhibitors, such as XIAP. Transfection of wild-type caspase 3 into various cell lines often has little or no effect on cell death, probably because the procaspase 3 does not self-activate efficiently. Overexpression generally does not lead to activation unless the protein concentrations are very high. We have shown, however, that it is indeed possible to activate procaspase 3 *in vitro* without cleavage of the IL, and transfection of the constitutively active mutant into cancer cells results in robust cell death.[10] The mutation of V266 to glutamate in the DI is thought to displace the IL and thus allow the substrate-binding pocket to form. In addition, the constitutively active variant is poorly inhibited by XIAP, which binds to the IL only when it is cleaved. Together, the data suggest that directly activating procaspase 3 through manipulating its conformational equilibria may provide novel strategies to kill cancer cells. Small molecule activators of procaspase 3 have been described,[11−13] although their mechanisms of activation are not entirely clear.[14,15]

Effector procaspases exist in equilibrium between active and inactive conformations,[10] and IL cleavage shifts the population toward the active form due to stabilizing the active site loops.[5,6] Structural studies of procaspase 7 showed that IL binding in the DI blocks formation of the active form due to steric constraints between regions of the IL and the substrate-binding loop.[16,17] It is thought that the ILs of caspases 3 and 7 are too short to allow efficient active site formation, suggesting that the active site can form only upon IL cleavage and removal from the DI. However, models of procaspase 3 indicate that the IL is sufficiently long to allow critical contacts in the active site loops if it were released from binding in the DI, thus explaining the constitutively active procaspase 3 variant.[10] The structural data suggested that lengthening the IL should result in an active caspase 3 (or 7) zymogen by relaxing the strain induced by a short IL. A recent study by Denault and colleagues[18] seemed to confirm this hypothesis. Although insertions of three Gly-Ser sequences (six residues) into the IL of procaspase 7 did not activate the zymogen, removal of several amino acids from the IL of procaspase 8 resulted in a zymogen that required cleavage for activation. Together, the structural, biochemical, and modeling data led to the prevailing view of an effector caspase zymogen that is sterically constrained, due to the short IL, which could form the fully active conformer only upon cleavage of the IL and its removal from the DI.

dx.doi.org/10.1021/bi400793s | *Biochemistry* 2013, 52, 6219−6231

In addition to the IL-lengthening model (Figure 1A), our data for the constitutively active procaspase 3[10] also suggested that a cluster of hydrophobic interactions in the DI, centered on V266, make specific contacts with residues in the IL (Figure 1C-D). The interactions may stabilize the inactive conformer by anchoring the IL in the interface. In the constitutively active variant, the mutation of V266 to Glu presumably disrupts the hydrophobic cluster.

In order to further examine the role of the IL in maintaining the inactive procaspase, we tested the two putative mechanisms for IL-mediated procaspase activation (Figure 1). For the active conformation (Figure 1A), we[19] and others[20,21] have shown that an important set of interactions occurs among active site loops 2, 2′, and 4, described as the loop bundle (Figure 1D). Disruption of these interactions dramatically reduces the activity of mature caspase 3. Although it was structurally feasible for the procaspase to adopt an active conformation with the intact IL, the IL was only just long enough to allow for the formation of the loop bundle at both ends of the dimer interface. According to this first model, therefore, increasing the length of the IL could lead to an increase in procaspase 3 activity by allowing the sampling of more conformational states that stabilize the loop bundle. To test this model, we increased the length of the IL of procaspase 3 through the insertion of up to eight alanine or glycine residues (Figure 1B). In the second model (Figure 1C), several hydrophobic residues in the IL stabilize its position in the DI, thereby favoring the inactive conformation. To test this model, we created mutants of procaspase 3 where one or more of the hydrophobic amino acids were replaced. We note that all variants described here were created in the background of the uncleavable procaspase 3, called D_3A, in which the three cleavage sites (D9, D28, D175) were mutated to alanine.[22] This strategy simplifies the interpretation since we are examining only the conformational equilibria of the procaspase and not the complete conformational states of cleaved/uncleaved protein. Results from activity assays and molecular dynamics (MD) simulations show a correlation between increasing the length of the IL and an increase in procaspase activity, while mutations in the hydrophobic cluster were less effective in activating the procaspase.

MATERIALS AND METHODS

Cloning, Protein Expression and Purification, Western Blots. Mutagenesis was performed as described previously[22] on the uncleavable procaspase 3 (D_3A) to obtain the single, double, and triple mutants described in this study. The single point mutants as well as the IL-lengthening mutants were first created using plasmid pHC33209[22] as a template. Subsequent mutants used those plasmids as a template. Primers and plasmid templates for each mutant are described in Supporting Information (SI) Table 1. The mutations were confirmed by sequencing both DNA strands.

E. coli BL21(DE3) pLysS cells were transformed with each plasmid, and the C-terminal His-tagged proteins were expressed and purified according to established protocols.[22,23] For cell culture experiments, the gene was cloned into pcDNA3.1(-) modified to contain a FLAG tag sequence at the C-terminus of the protein.

Western blots were carried out as described,[10] with the following modifications. Equal amounts of each sample (6.5 μg purified protein) were subjected to SDS-PAGE (12.5%) and transferred to a nitrocellulose membrane. The membrane was blocked using 5% milk powder in 1X TBS with 0.1% Tween 20 for 20 min at 4 °C. The membrane was probed using purified mouse anti-human caspase 3 (1:1000) (BD Biosciences) overnight at 4 °C in blocking buffer. Visualization of caspase 3 mutants was performed using ECL horseradish peroxidase (HRP)-conjugated sheep antimouse IgG (1:4000) in blocking buffer and enhanced chemiluminescence blotting reagents (GE Healthcare).

Enzyme Activity Assays. The initial velocity of substrate cleavage was measured at 25 °C in the presence of varying concentrations of substrate (Ac-DEVD-afc), as described previously.[22,24] The final protein concentration for the active mutants was 10 nM, whereas a protein concentration of 100 nM or 400 nM was used for the largely inactive mutants. The total reaction volume was 200 μL. Briefly, substrate was added to the sample that contained protein in activity assay buffer (150 mM Tris−HCl, pH 7.5, 100 mM DTT, 0.1% CHAPS, 50 mM NaCl, 10% sucrose), and samples were immediately excited at 400 nm while the fluorescence emission was measured at 505 nm for 60 s. Plots of the initial velocity versus substrate concentration were fit to the Michaelis−Menten equation to obtain the steady-state parameters, K_M and k_{cat}.

Inhibition studies were carried out using the following protocols. Working stocks of inhibitors (Z-VAD-fmk or Ac-DEVD-cmk) were made by dilution in activity assay buffer, and the stock solution (20 μL) was added to protein solution (180 μL) for a final protein concentration of 100 nM. The final inhibitor concentration varied from 2 nM to 800 nM, as shown in the figures, and samples were incubated at 25 °C for 1 h. Following incubation, substrate was added (0 and 100 μM for data in Figure 4A; 20 μM for active site titrations), and samples were immediately excited at 400 nm while fluorescence emission was measured at 505 nm for 60 s. Plots of initial velocity versus substrate cleavage at each inhibitor concentration (Figure 4A) or initial velocity versus inhibitor concentration (active-site titrations) were either fit to the Michaelis−Menten equation to obtain V_{max} or linear extrapolation to obtain the concentration of active sites.

Identification of Cleavage Sites by Mass Spectrometry. Proteins were dialyzed in a buffer of 20 mM KH_2PO_4/K_2HPO_4, pH 7.2, 1 mM DTT and were used to prepare samples in 0.1% formic acid at a protein concentration of 0.5 μM. Samples were stored at −20 °C until analyzed.

For intact protein molecular weight measurements (top down analysis), samples were analyzed by liquid chromatography−mass spectrometry (LC/MS) using a NanoAcquity ultrapressure liquid chromatography (UPLC) system (Waters Corporation) coupled to a Q-Tof Premier quadrupole time-of-flight mass spectrometer (Waters Corporation). Protein components were separated using a column (75 μm i.d. × 25 cm) packed with BEH C18 particles (1.7 μm, Waters Corporation) by running a gradient of water and acetonitrile containing formic acid. The outlet of the UPLC column was connected directly to the nanoelectrospray source of the Q-Tof. Positive ion mass spectra were acquired over the range of either 400−2000 m/z or 800−3500 m/z at a rate of 1 scan/s. Raw LC/MS data were reviewed manually for evidence of protein charge state envelopes, and observed charge state envelopes were deconvoluted using the MaxEnt 1 module contained in the MassLynx 4.0 acquisition software to convert m/z scale mass spectra to molecular weight scale data. The Biolynx module within MassLynx was used for comparison of observed molecular weights against various mutant caspase sequences.

For analysis of inhibited protein by mass spectrometry, the protein sample (25 μM) was incubated with inhibitors (Ac-

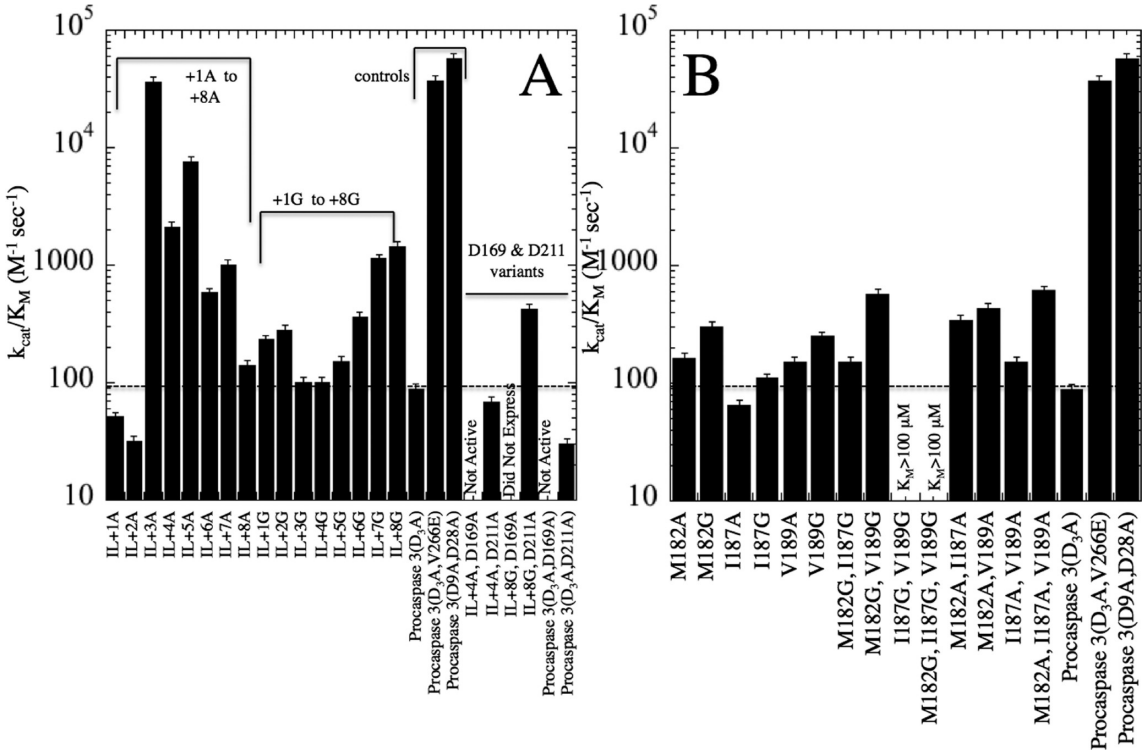

Figure 2. Enzyme activity assays. (A) Activity of IL insertion mutants +1A to +8A and +1G to +8G. (B) Activity of hydrophobic cluster mutants. For panels A and B, procaspase 3(D_3A) is the uncleavable variant (D9A,D28A,D175A) and represents background activity of the procaspase (dashed lines). Procaspase 3(D_3A,V266E) is an uncleavable constitutively active variant described previously,[10,33] and procaspase 3(D9A,D28A) represents a cleavable procaspase that retains the pro-peptide.[32]

DEVD-cmk (550.94 Da) or Z-VAD-fmk (453.46 kDa); 200 μM final concentration) for 1 h at 25 °C in a buffer of 20 mM phosphate, pH 7.2, 1 mM DTT. For LC/MS analysis, a 1:50 dilution of the incubation was made using the same buffer, yielding a final protein concentration of 0.5 μM. Samples were analyzed using the top down procedure described above.

Generation of Structural Models and Molecular Dynamics Simulations. Model structures for the insertion mutants were generated using the online tool Swiss-Model[25−27] in the automated mode, using either the active or inactive procaspase 3 homology model as the template.[10] Modeling was performed for each monomer separately, and the resulting files were merged to create the structure for the dimer. For the hydrophobic mutants, the models of inactive and active procaspase 3 were mutated *in silico* using Pymol.

Molecular dynamics simulations were performed as described previously[28] with GROMACS 4.5,[29] using the Amber99 force field[30] and the tip3p water model.[31] The models generated using the method described above were used as the initial structures for the simulations, which were performed for each mutant in both the active and inactive conformations. Energy minimization was performed for each structure using steepest descent. Simulations of 50 ns were run with a time step of 2 fs and coordinates were saved every 5 ps.

RESULTS

A Longer IL Leads to Increased Enzyme Activity in the Zymogen. According to the first model (Figure 1A), in the absence of other factors that stabilize the inactive form, increasing the length of the IL of procaspase 3 should allow the enzyme to sample more states in the active conformation. A longer IL would presumably stabilize the loop bundle (Figure 1D), despite the lack of IL cleavage, similar to what may occur for initiator procaspases upon dimerization. To test this model, we inserted up to eight alanine or glycine amino acids (called +1A to +8A, and +1G to +8G) into the IL of the uncleavable procaspase 3(D_3A). We placed the insertions at a site in the IL that contains several additional residues in procaspase 8 (between V178 and D179), as indicated by sequence alignment, and N-terminal to the proposed hydrophobic cluster (Figure 1B and D). In addition, H185 and residues C-terminal to H185 are important in stabilizing the loop bundle, so the insertions were placed N-terminal to these residues.

Activity assays show that insertion of one or two alanines had little effect on enzyme activity compared to the background of procaspase 3(D_3A) (Figure 2, SI Table 2). There was a large increase, however, upon insertion of three or more alanines, where the k_{cat}/K_M values were >10^4 M^{-1} s^{-1} for the +3A variant. The activity can be compared to a value of 1.8×10^5 M^{-1} s^{-1} for wild-type, cleaved, caspase 3,[24] 5.7×10^4 M^{-1} s^{-1} for the D9A,D28A variant,[32] and 3.7×10^4 M^{-1} s^{-1} for the constitutively active procaspase 3(D_3A,V266E) variant[33] (Figure 2A). The D9A,D28A double mutant, described previously,[32] results in a caspase that is cleaved at D175 in the IL but that retains the pro-domain. The +3A, +4A, and +5A variants were approximately 100-fold more active than procaspase 3(D_3A). We also note that activity decreased with >5 alanine insertions, where the +8A variant exhibited activity close to that of the background procaspase 3(D_3A). This feature is discussed more fully below.

For the glycine insertions, introduction of one to five glycines had little effect on activity (Figure 2), as the data show that the mutants have activities similar to that of procaspase 3(D_3A). With insertions of five or more glycines, however, the activity increased systematically. The addition of seven or eight glycines

dx.doi.org/10.1021/bi400793s | *Biochemistry* 2013, 52, 6219−6231

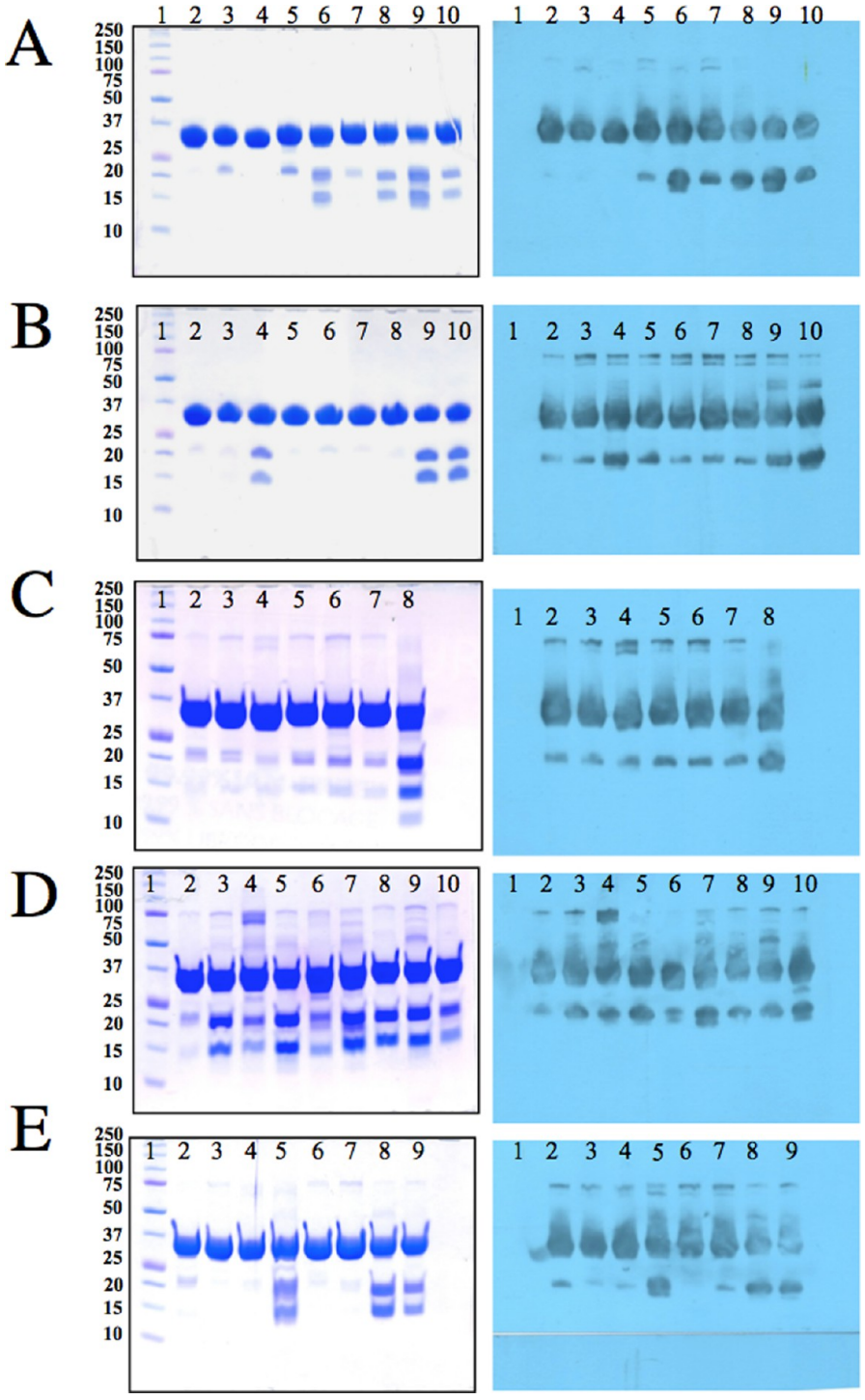

Figure 3. SDS-PAGE (left panels) and Western analyses (right panels) of IL mutants. (A) +A series. Lane 1: molecular weight markers; lane 2: procaspase 3(D_3A); lane 3: +1A; lane 4: +2A; lane 5: +3A; lane 6: +4A; lane 7: +5A; lane 8: +6A; lane 9: +7A; lane 10: +8A. (B) +G series. Lane 1: molecular weight markers; lane 2: procaspase 3(D_3A); lane 3: +1G; lane 4: +2G; lane 5: +3G; lane 6: +4G; lane 7: +5G; lane 8: +6G; lane 9: +7G; lane 10: +8G. (C) Hydrophobic cluster mutants, single. Lane 1: molecular weight markers; lane 2: procaspase 3(D_3A); lane 3: M182A; lane 4: M182G; lane 5: I187A; lane 6: I187G; lane 7: V189A; lane 8: V189G. (D) Hydrophobic cluster mutants, multiple. Lane 1: molecular weight markers; lane 2: procaspase 3(D_3A); lane 3: M182G,I187G; lane 4: M182A,I187A; lane 5: M182G,V189G; lane 6: M182A,V189A; lane 7: I187G,V189G; lane 8: I187A,V189A; lane 9: M182G,I187G,V189G; lane 10: M182A,I187A,V189A. (E) Alternate cleavage site variants. Lane 1: molecular weight markers; lane 2: procaspase 3(D_3A); lane 3: D_3A,D169A; lane 4: D_3A,D211A; lane 5: +4A; lane 6: +4A,D169A; lane 7: D_3A,D211A; lane 8: +8G; lane 9: +8G,D211A. All mutations are in the background of procaspase 3(D_3A).

resulted in activity >10^3 M^{-1} s^{-1}, approximately equivalent to the +6A and +7A variants.

Disrupting the Hydrophobic Cluster Has Little Effect on the Activity of Procaspase 3. According to the second model (Figure 1C), the position of the IL in the DI is favored through hydrophobic interactions (Figure 1D), which act to stabilize the inactive conformation. If the model is correct, then replacing these residues would destabilize the inactive con-

dx.doi.org/10.1021/bi400793s | *Biochemistry* 2013, 52, 6219−6231

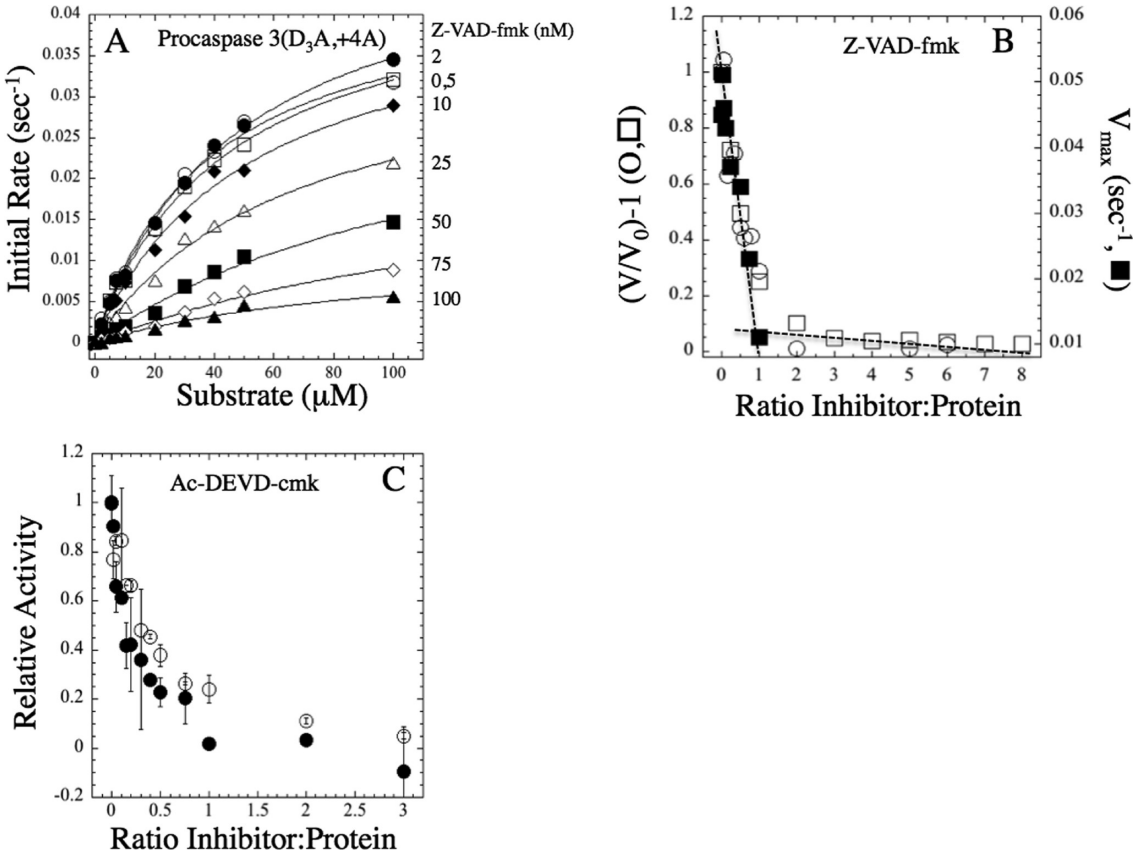

Figure 4. Enzyme inhibition and active site titrations. (A) Initial rates of procaspase 3(D_3A,+4A) were determined following incubation with Z-VAD-fmk (0−100 nM) at a substrate concentration of 20 μM. Data were fit to the Michaelis−Menten equation (solid lines) to determine V_{max}. (B) Active site titration of procaspase 3(D_3A) (○) and procaspase 3(D_3A,+4A) (□) in the presence of Z-VAD-fmk inhibitor. V_{max} values for procaspase 3(D_3A,+4A) (■) were from panel A. Dashed lines do not represent fits to the data but rather show maximum inhibition occurs at an inhibitor to protein ratio of ~1:1. (C) Active site titration of procaspase 3(D_3A) (○) and procaspase 3(D_3A,+4A) (●) in the presence of Ac-DEVD-cmk inhibitor. For A−C, protein concentrations were 100 nM.

formation and shift the procaspase 3 equilibrium toward the active conformer. To test this model, we mutated each of the three hydrophobic residues, namely, M182, I187, and V189 (Figure 1D), to either alanine or glycine, either singly or in combination (see SI Table 1).

As shown in Figure 2B, single mutations to either alanine or glycine had little effect on activity. We observed an approximate 2-fold change for some mutants and little or no change for others. For the double mutants, there was an increase in activity of approximately 3-fold, and the triple mutation, where the three residues were replaced with alanine, resulted in an increase in activity of about 6-fold. For most of the mutants, the changes were independent of whether the residue was replaced with glycine or alanine. We note that the I187G,V189G double mutant and the M182G,I187G,V189G triple mutant had very high K_M values, so we were unable to measure the k_{cat} or k_{cat}/K_M values of those variants (Figure 2B). At present, it is unclear why the two mutants have low activity. Overall, the activities for the hydrophobic cluster variants are well below that of the V266E constitutively active procaspase 3. The data show that disrupting the interactions does not result in a significant increase in enzyme activity for the procaspase, so the hydrophobic cluster is not important for maintaining the inactive conformation of procaspase 3.

IL Mutations Result in Minor Populations of Alternately Cleaved Inactive Protein. Although procaspase 3 is not a good substrate for self-cleavage, the enzyme is known to self-process when expressed in *E. coli* at high protein concentrations. Because the three processing sites, D9, D28, and D175, were mutated to alanine in our mutants, we did not expect self-processing of the recombinant proteins at those sites. We could not, however, rule out minor cleavage reactions at alternative sites. In order to assess alternate cleavage of the IL mutants, we examined concentrated protein samples by SDS-PAGE. The results show that procaspase 3(D_3A) has a minor cleavage product of ~19 kDa (lane 2 in Figure 3A-D, left panels). All mutants, with the exception of the +2A variant (Figure 3A, lane 3), demonstrated the same band at ~19 kDa, with more of the product present (Figure 3B-D). In addition, a less prevalent product of ~23 kDa was present in several of the mutants. Western analyses of the proteins showed that the ~19−23 kDa species correspond to alternate cleavages in the large subunit of procaspase 3 (Figure 3A-D, right panels).

We investigated the possibility that the increase in enzyme activity observed for the variants (Figure 2) was due to the presence of the alternately cleaved procaspase by performing inhibition studies with the pan-caspase inhibitor Z-VAD-fmk. We examined the +4A mutant because it demonstrated high activity (Figure 2A) and increased cleavage compared to the control of procaspase 3(D_3A) (Figure 3A, lane 6 versus lane 2). The IL variant was incubated with various concentrations of inhibitor, and then enzyme activity was determined at several substrate concentrations (Figure 4A). Each activity profile was fit to the Michaelis−Menten equation, and V_{max} was plotted versus

dx.doi.org/10.1021/bi400793s | *Biochemistry* 2013, 52, 6219−6231

Table 1. Alternate Cleavage Site Determined by Mass Spectrometry

mutant	full-length		alternate cleavage at TELD(169): large subunit		alternate cleavage at TELD(169): small subunit (Da)	
	calculated (Da)	experimental (Da)	calculated (Da)	experimental (Da)	calculated (Da)	experimental (Da)
Procaspase-3 (D9A,D28A,D17 5A) (AKA, D_3A)	32541.09	32539.63 ± 8.2	19023.67	19022.71 ± 2.90	13535.43	13533.77 ± 10.13
Procaspase-3 (D_3A,+1A)	32612.17	32609.33 ± 0.51	19023.67	ND	13606.51	ND
Procaspase-3 (D_3A,+2A)	32683.25	31851.20 ± 1.18	19023.67	19025.03 ± 8.03	13677.59	ND
Procaspase-3 (D_3A,+3A)	32754.33	ND	19023.67	ND	13748.67	13746.15 ± 0.64
Procaspase-3 (D_3A,+4A)	32825.41	32823.09 ± 2.75	19023.67	19021.78 ± 0.74	13819.75	ND
Procaspase-3 (D_3A,+5A)	32896.48	32900.54 ± 12.82	19023.67	19021.97 ± 0.67	13890.82	ND
Procaspase-3 (D_3A,+6A)	32967.56	32967.20 ± 8.65	19023.67	19021.78 ± 0.11	13961.90	ND
Procaspase-3 (D_3A,+7A)	33038.64	33035.66 ± 0.39	19023.67	19022.87 ± 0.36	14032.98	14031.26 ± 1.66
Procaspase-3 (D_3A,+8A)	33109.72	33113.95 ± 15.33	19023.67	19021.39 ± 0.55	14104.06	ND
Procaspase-3 (D_3A,V189G)	32499.01	32498.14 ± 19.19	19023.67	19021.61 ± 1.16	13493.35	13489.11 ± 3.95
Procaspase-3 (D_3A) + Ac-DEVD-cmk	33056.49	33053.35 ± 13.98 (64% labeled)	19539.61	19537.12 ± 9.70 (78% labeled)		
Procaspase-3 (D_3A) + Z-VAD-fmk	32989.49	32996.36 ± 20.21 (22% labeled)	19472.16	19471.0 ± 11.36 (81% labeled)		
Procaspase-3 (D_3A,+4A) + Ac-DEVD-cmk	33340.49	33341.ll ±15.04 (83% labeled)	19539.61	19539.76 ± 5.14 (84% labeled)		
Procaspase-3 (D_3A,+4A) + Z-VAD-fmk	33273.49	33271.88 ± 15.39 (38% labeled)	19472.16	19464.66 ± 9.01 (93% labeled)		

inhibitor (Figure 4B, closed symbols). We also performed active site titration studies of procaspase 3(D_3A) and the +4A variant with Z-VAD-fmk (Figure 4B, open squares and circles, respectively). Together, the data show that the inhibitor binds to each protein in a 1:1 stoichiometry with the total number of active sites.

In addition to the pan-caspase inhibitor, we performed active site titrations of the two proteins with Ac-DEVD-cmk inhibitor, which contains the consensus cleavage site for caspase 3. As shown in Figure 4C, the data were nearly identical for the two proteins even though the activity of the +4A variant is much higher than that of the control. The titrations show that the inhibitor binds with a stoichiometry of ~0.5:1 (inhibitor:active sites), suggesting that the two active sites in the dimer may not be equivalent. This feature was not observed with the shorter sequence, Z-VAD-fmk.

If the increase in enzyme activity, described above (Figure 2), were due only to the alternately cleaved protein, then one would observe a binding stoichiometry much less than 1:1 or 0.5:1 (inhibitor to total active sites). That is, the active site titrations would reflect only the active protein, and the data in Figure 3 show that the alternately cleaved protein is present at low levels compared to the full-length protein. One cannot explain the observed binding stoichiometry unless the inhibitors bind to the full-length proteins, so we conclude that the activity observed for each protein reflects the intrinsic activity of the full-length procaspase. Finally, the trends in the activity profiles do not correlate with the levels of the minor cleavage products. For example, the +5A variant (Figure 3A, lane 7) has higher activity but less alternately cleaved large subunit than does +7A (Figure 3A, lane 9). Likewise, the V189G single mutant has similar activity to that of the M182A,I187A double mutant (Figure 2B) but significantly more cleavage (compare Figure 3C, lane 8, to Figure 3D, lane 4).

We determined the alternate cleavage sites that produced the ~19 kDa product using liquid chromatography-tandem mass spectrometry (LC/MS/MS) on intact protein samples (Table 1). In these studies we examined procaspase 3(D_3A) (Figure 3A-E, lane 2), the +1A to +8A variants (Figure 3A, lanes 2−10), and the V189G variant (Figure 3C, lane 8). The data were consistent for all proteins examined and showed that the large subunit is cleaved at D169 (TELD) to produce a fragment of 19 023 Da. The calculated size of the large subunit cleaved at D169, while retaining the pro-domain, is 19 024 Da, and this fragment was observed for all of the proteins with the exception of the +1A variant (Table 1). The ~23 kDa fragment was not observed by mass spectrometry, but the data in Figure 3 are consistent with cleavage at D211 (NSKD), which produces a fragment of 23.8 kDa. Overall, the data shown in Figure 2 and summarized in Table 1 are consistent with a self-cleavage at two alternate sites: D169 and D211.

Although D169 is upstream of the normal cleavage site (D175) in the IL of procaspase 3, the side-chain has been shown to be important for stabilizing the "loop bundle", and hence the active site, in the mature, cleaved, caspase.[19,20] In addition, we have suggested that D169 is important in stabilizing the active conformation of the constitutively active procaspase 3 (Figure 1D and ref 10). In contrast, D211 is located in loop 3, which forms the base of the substrate-binding pocket (Figure 1). We replaced each of the two residues individually with alanine (D169A and D211A) in the context of procaspase 3(D_3A), the +4A variant (Figure 3A, lane 6), and the +8G variant (Figure 3B, lane 10), and we examined the enzyme activity as well as the presence of alternately cleaved protein by SDS-PAGE and Western blots. The results show that mutation of D169 to alanine in the uncleavable procaspase(D_3A) or the +4A variant abolished enzyme activity (Figure 2A). The +8G,D169A variant did not express in our *E. coli* expression system, so we could not examine the activity of this protein (Figure 2A). In contrast, the D211A mutation had less effect on the activity, where the activities of the variants were similar to that of procaspase 3(D_3A) (Figure 2A).

Examination of the variants by SDS-PAGE showed that the levels of alternately cleaved protein were substantially decreased when either D169 or D211 was replaced with alanine (Figure 3E, left panel). Western analyses confirmed that there were significantly lower amounts of the alternately cleaved protein (Figure 3E, right panel). In the +8G,D211A variant (Figure 3E, lanes 8−9), cleavage at D169 appears to be the primary site of

dx.doi.org/10.1021/bi400793s | *Biochemistry* 2013, 52, 6219−6231

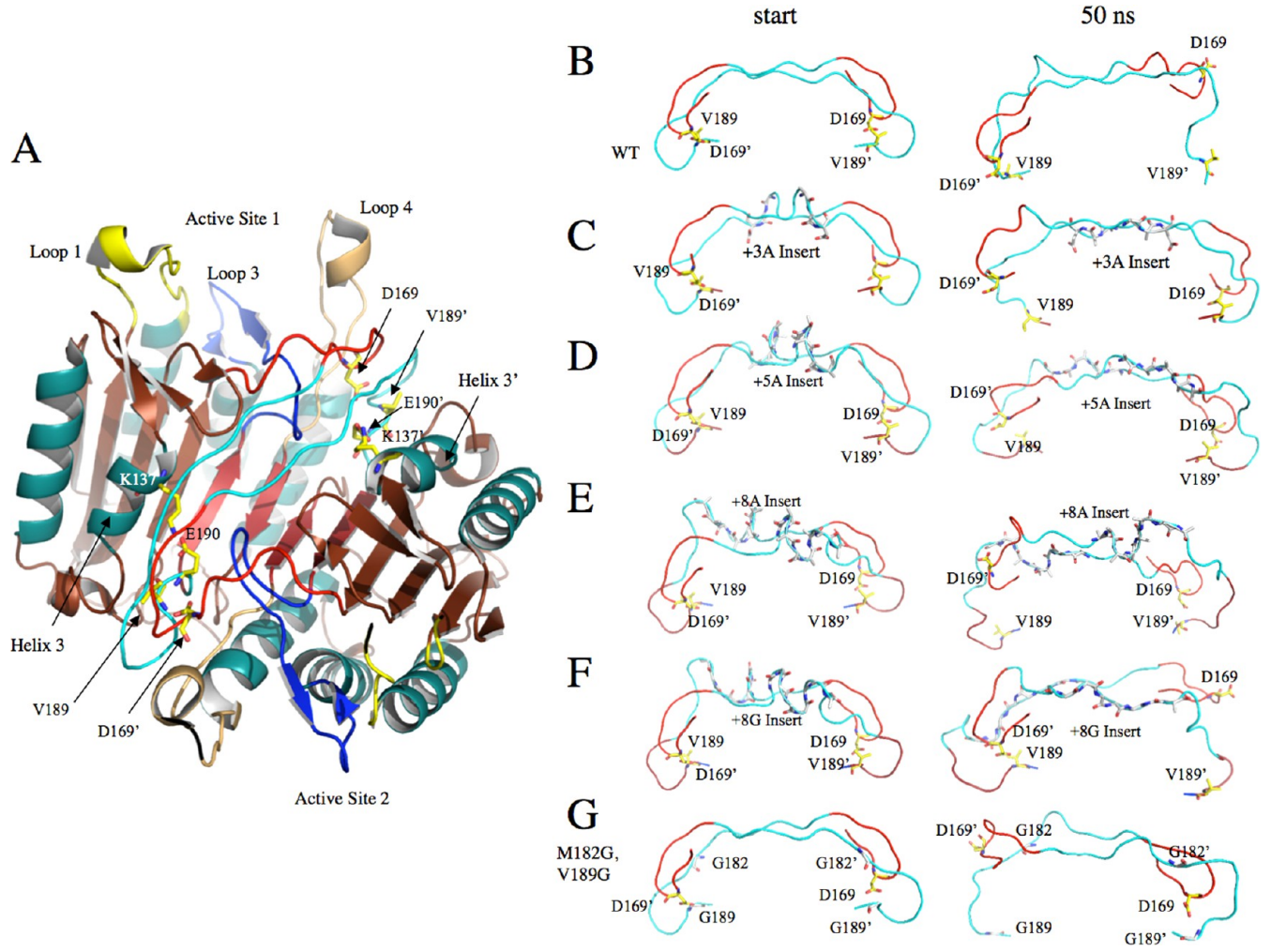

Figure 5. Molecular dynamics simulations of the active conformer of procaspase 3. (A) Model for the active (starting) conformation of procaspase 3. The two active sites and intersubunit linkers are labeled. Amino acids V189, D169, K137, and E190 are shown in yellow sticks for each monomer. The prime (′) indicates amino acids from the second monomer. (B−G) IL conformations for starting (left) and ending (50 ns, right) structures for (B) procaspase 3(D_3A) (AKA, wild-type or WT), (C) +3A, (D) +5A, (E) +8A, (F) +8G, and (G) M182G,V189G. In panels B−G, loop bundle interactions are indicated by the V189-D169′ pair. Changes in distances between the side chains are shown in Figure 6.

alternate cleavage since the cleavage observed remains significant. Overall, the collective data show that D169 and D211 represent alternate cleavage sites when the primary site for activation, D175, is not available. The data suggest that D169 is the major site of alternate cleavage, whereas D211 is a minor site.

Taken together, the results presented here provide strong evidence that the increase in activity observed for the procaspase 3 variants is due to changes in the IL rather than to the minor cleavage products. This conclusion is consistent with our previous studies of the constitutively active V266E variant of procaspase 3[10] using an active site label. In those studies, the probe labeled the active site of the full-length procaspase, demonstrating the observed activity was due to the uncleaved procaspase. In addition, little or no cleavage was observed for that protein by Western analysis. We also note that we previously examined the single mutant procaspase 3(D169A)[19] and showed that the mutant was inactive and unprocessed, even though the three cleavage sites were intact (D9, D28, D175). Likewise, the caspase 3(D169A) variant also demonstrated little to no activity.[19] The side chain of D169 forms hydrogen bonds with backbone amides of V189′ and E190′ from the second monomer, and the interactions are critical for stabilizing the loop bundle of the active enzyme (see Figure 1D). Our current and previous results show that the alternate cleavage at D169 (and probably D211) occurs by a self-cleavage event, but the product is likely to be enzymatically inactive due to disruption of contacts in the loop bundle.

Molecular Dynamics Simulations Show Increased Flexibility in the IL of Insertion Mutants. In order to further understand why the +3A to +5A insertions resulted in robust increases in activity while other insertions did not, we performed molecular dynamics simulations for each of the insertion mutants, as well as for the uncleavable procaspase 3, for a total length of 50 ns. We used the models for active as well as inactive procaspase 3 (with and without the insertions) (see Figure 1A,B) as starting structures for the simulations because previous results showed that the two structures do not interconvert within the time scale of the simulation.[28] Thus, we wished to examine interactions in each structure that may stabilize the active or inactive ensembles, respectively, and how those interactions changed as a result of the insertion. Over the course of the simulations, overall structures were largely similar to that of the crystal structure for mature caspase 3 (less than 7 Å RSMD for the backbone, or within 5 Å RMSD of the starting models).

dx.doi.org/10.1021/bi400793s | *Biochemistry* 2013, 52, 6219−6231

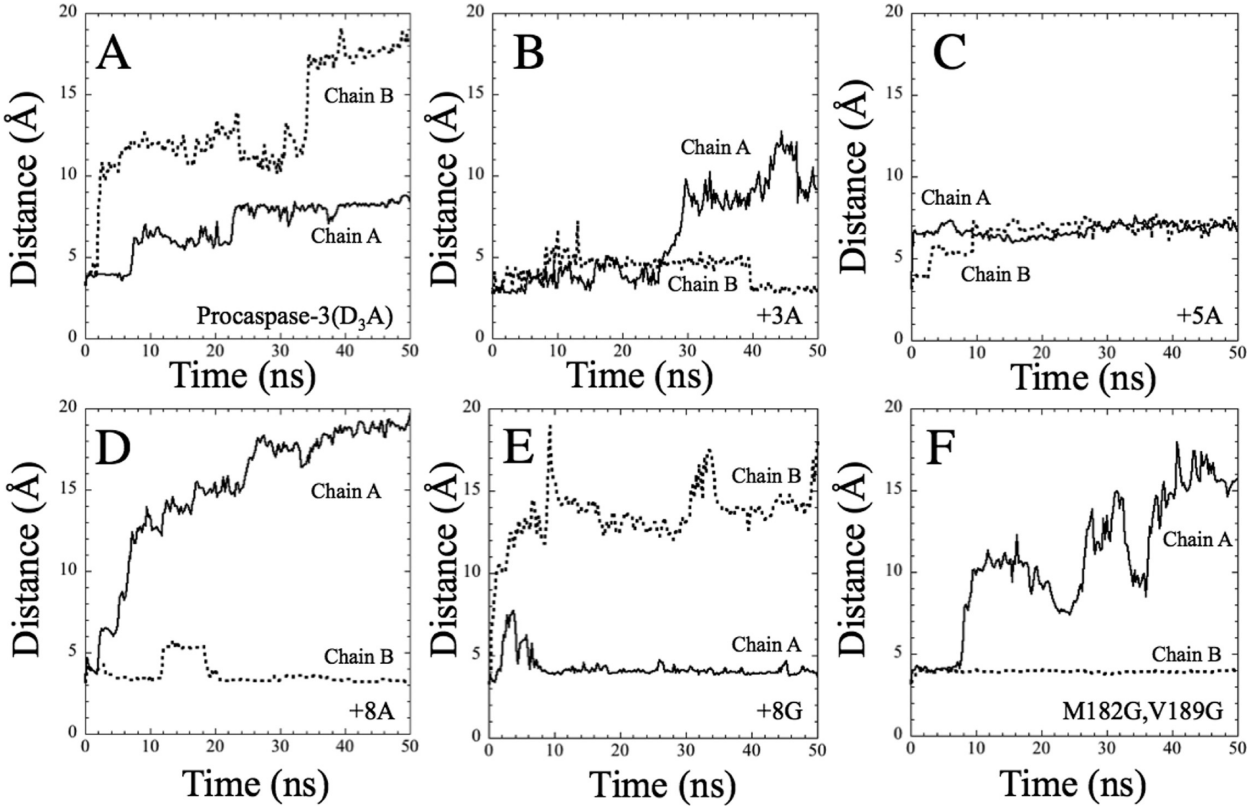

Figure 6. Distance calculations from molecular dynamics simulations. Distances between D169 (side chain δO) and the backbone amide of V189′ for monomer A (chain A, solid line) or monomer B (chain B, dashed line) in the procaspase 3 dimer. (A) procaspase 3(D_3A), (B) +3A, (C) +5A, (D) +8A, (E) +8G, (F) M182G,V189G. Simulations were performed for 50 ns as described in the text. All mutations are in the background of procaspase 3(D_3A).

Simulations utilizing the model for inactive procaspase 3 (uncleavable D_3A and insertion mutants) demonstrated that the IL remained bound to the dimer interface over the time course of the simulation (data not shown), so these results are not discussed further. Rather, we focus here on results for the active conformers.

We consider changes in the interactions between D169 (side chain δO) and the backbone amide of V189′, as well as interactions between E190 (side chain εO) and K137 (side chain ζN), to monitor stability of the loop bundle and flexibility in the IL and helix 3 (Figure 5A). In the case of uncleavable procaspase 3(D_3A) (without insertions), results show a rapid loss of key interactions known to be important for active site stabilization. The same interactions were shown previously to be maintained in mature caspase 3.[28] For example, distances between D169 and V189′ increased from ∼4 Å to ∼18 Å (chain B or monomer B) or ∼9 Å (chain A or monomer A) (Figure 5B and Figure 6A). Distances between these two atoms of ∼4 Å represent a correctly formed active site and stable loop 4 (see Figure 5A), while the longer distances represent a very flexible IL. At the end of the 50 ns simulation, the side chain of D169 from one IL (monomer B) was completely exposed to solvent (Figure 5B, right panel). The distance between K137 and E190 also increased to ∼18 Å for chain B (SI Figure 1A). These results suggest that the loop bundle interactions are not stable in the active procaspase-3 conformer and are consistent with our previous data that show the inactive ensemble of procaspase 3 is favored.[13,28] The low activity of wild-type procaspase 3 is likely a reflection of the relative population of inactive (favored) and active (disfavored) conformers within the ensemble of native protein. Overall, the results of the MD simulations of active procaspase 3 show that the protein undergoes numerous structural changes that impact active site formation, particularly in formation of the loop bundle and stabilization of helix 3. In contrast, mature (cleaved) caspase 3 remains largely in the active conformation.[28]

Several differences were observed in simulations of the IL mutants. For clarity, data are presented in Figures 5 and 6 (and SI Figure 1) for the +3A, +5A, +8A, +8G, and M182G,V189G variants for the following reasons. The +3A and +5A variants demonstrated robust increases in enzyme activity, while the activity of the +8A mutant was similar to that of procaspase 3 (Figure 2). The activity of the +8G variant was ∼10-fold higher than that of +8A, and the M182G,V189G double mutant demonstrated the highest activity of the hydrophobic cluster series, although the activity was significantly lower than most of the IL insertion mutants.

For the +3A and +5A variants, the loop bundle remained largely intact, as observed by the distances between D169 and V189′ and between K137 and E190. For +3A, D169 and V189′ were within ∼4 Å for at least half of the simulation, and the side chains were between ∼4 Å (chain B) or ∼10 Å (chain A) throughout the simulation (Figure 5C, Figure 6B, SI Figure 1B). In the case of the +5A variant, the D169-V189′ pair remained within 7 Å of each other throughout the simulation (Figure 5D and Figure 6C), while the K137-E190 pair were within 5 Å (SI Figure 1C). Together, the data suggest that the two proteins are active because the insertion of three to five alanine residues stabilizes the loop bundle as well as helix 3, in both monomers, thus shifting the ensemble to the active conformer. In contrast, the data for the +8A variant more closely resemble those of procaspase 3(D_3A). One IL appears to be very flexible (Figure 5E, also compare Figures 6A and D and SI Figures 1A and 1D),

dx.doi.org/10.1021/bi400793s | *Biochemistry* 2013, 52, 6219−6231

although in general the distances for the second monomer are shorter in this mutant compared to those of the control.

The data for the +8G variant are similar to those of the +3A and +5A variants except that one active site appears to be stabilized while the second active site is not. In this protein, the distance between D169 and V189′ in monomer A remains constant at ∼4 Å, while the distance increases to ∼15 Å in monomer B (Figure 5F and Figure 6E). Likewise, the distance between K137 and E190 (∼4 Å in monomer Å and ∼13 Å in monomer B) shows that the IL is stabilized in one monomer but not the other (SI Figure 1E). Thus, the intermediate level of enzyme activity for this variant (Figure 2) may be due to stabilization of only one active site in the dimer.

The double mutant, M182G,V189G, is intermediate between procaspase3(D_3A) and the +5A variant (Figure 5G, Figure 6F, and SI Figure 1F). In this mutant, the D169-V189′ pair remains close for one monomer, within ∼4 Å, but the pair demonstrates large flexibility in the second monomer, where the distance is ∼15 Å (Figure 6F). In addition, the K137-E190 pair has increased flexibility for both monomers, where distances increase to ∼11 Å (SI Figure 1F). The data suggest that the activity of this mutant may be lower because of increased flexibility in the IL compared to the +3A or +5A insertion mutants.

Overall, results from the MD simulations are consistent with a flexible IL in the uncleavable procaspase 3(D_3A) that results in a destabilized loop bundle and active site. Lengthening the IL by 3−5 alanine residues stabilizes the loop bundle in one or both active sites, and the new contacts that form in the loop bundle (that is, the active conformer) likely decreases flexibility overall in the IL. Longer insertions appear to affect one active site while the second active site remains flexible. For the +6A to +8A variants, flexibility in the IL may also be affected by formation of 1−2 turns of helix in the longer IL (see Figure 5E, right panel), which overall shortens the IL and moves D169 away from V189′. In addition, formation of secondary structure in the IL may be important for positioning D169 close to V189′, since the more flexible glycine insertions show much lower activities than the equivalent alanine insertions.

DISCUSSION

Our previous data showed that the procaspase 3 native state ensemble contains at least two conformations, one of which is enzymatically active while the other is inactive.[10,13] As with other effector procaspases, the inactive conformer of procaspase 3 is favored, as evidenced by the low endogenous activity. Previous mutational studies in the DI have shown that the active conformer is populated when the IL is expelled from its binding in the DI, and the constitutively active procaspase 3 supports robust cell death in cancer cells.[10] This view of the procaspase 3 conformational ensemble is in contrast to the prevailing view in which cleavage of the IL is required for the structural rearrangements needed for active site formation,[15] although the activation-by-cleavage mechanism certainly is the case *in vivo* as it affords tight control of apoptosis. The work we present here shows that, while cleavage of the IL results in full activation of procaspase 3, it is not required to activate the zymogen. Rather, stabilizing the active conformer of the procaspase, in the absence of chain cleavage, also generates an active procaspase, albeit at lower activity than the cleaved form.

Based on our previous work on procaspase 3 (ref 10) and structural data for procaspase 7 (refs 16,17), we proposed two models to explain how the IL is involved in maintaining the inactive conformation (Figure 1). The first model (IL-extension) states that lengthening the IL to more closely resemble initiator procaspases, such as procaspase 8, should increase the population of active conformer within the native ensemble by allowing the zymogen to sample more conformational states. In essence, the shorter IL in effector caspases constrains the native ensemble and limits the ability of the protein to maintain certain interactions known to play a role in the activity of the mature caspase (the loop bundle, for example). Indeed, Denault and co-workers recently showed that a procaspase 8 variant with a truncated IL requires cleavage for activation.[18] Ordinarily, procaspase 8 activation occurs upon dimerization on death scaffolds and does not require chain cleavage,[3] so their data imply that the shorter IL in the procaspase 8 variant mimics that of an effector procaspase. In contrast to the first model, the second model we proposed for maintaining the inactive procaspase 3 states that the inactive conformation is stabilized through hydrophobic interactions between the IL and the DI. The second model predicts that weakening the binding of the IL in the interface by disrupting the hydrophobic cluster should favor formation of the active conformer.

To test the IL-extension model, we made insertions of up to eight alanine or glycine residues in the IL of uncleavable procaspase 3(D_3A), and to test the hydrophobic cluster model, we mutated three sites in the IL that are predicted to interact with the DI. The data show that the IL maintains the inactive conformation by constraining the protein in a way to prevent key interactions that stabilize the active site. Removing interactions in the hydrophobic cluster (M182, I187, V189; see Figure 1D) had little effect on activity of the procaspase (Figure 2). In contrast, increasing the length of the IL by inserting 3−5 alanine residues resulted in a robust increase in enzyme activity. Molecular dynamics simulations of the mutants suggest that the modest increase in length allows interactions to form in the loop bundle, thus stabilizing the active conformer. Longer insertions, as with the +6A to +8A variants, resulted in ILs with increased flexibility and secondary structure formation, leading to suboptimal interactions in the loop bundle. At present, it is not clear why the +G insertions differ from the +A series, as the increase in activity was not observed until >6 glycines were added. Overall, however, the data show that releasing the strain of the short IL in procaspase 3, in and of itself, is not sufficient to populate the active conformer of the native ensemble. The IL must also allow for stabilizing interactions in the loop bundle, possibly from a combination of optimal length, secondary structure and/or flexibility in the IL, and specific contacts between the IL and DI. Our results may explain why no increase in activity was observed for procaspase 7 upon insertion of six residues in the IL (three GS pairs).[18] In that case, the inserted residues likely do not provide an optimal length.

Based on results from active site inhibition measurements with Ac-DEVD-cmk and from mass spectrometry, Wells and co-workers concluded that the activity observed in procaspase 3 arises from small amounts of cleaved protein in the sample.[15] In those studies, the authors primarily examined the wild-type procaspase 3, where the protein is most likely cleaved at D175. In that case, the contaminating cleaved product would be expected to exhibit much higher activity than the zymogen, equivalent to the procaspase 3(D9A,D28A) variant, which has been shown to have high enzyme activity.[32] In the work presented here, we examined the uncleavable procaspase 3(D_3A) variant, which removes the cleavage site at D175. We show that when D175 is not available for processing, the zymogen is cleaved at an alternate cleavage site (D169), but the minor cleavage product is

enzymatically inactive because D169 is important for maintaining the loop bundle contacts in the active protein (see Figure 1D). The alternate cleavage site at D169 becomes more exposed in several of the IL mutants, so more of the alternatively cleaved protein is observed in those mutants. Active site titrations with Z-VAD-fmk and Ac-DEVD-cmk inhibitors show that the full-length protein is active, and we observed by mass spectrometry that the inhibitor labels the full-length protein. Together, our data show that the protein cleaved at D169 has little to no enzyme activity and that the intrinsic activity of the uncleavable procaspase 3(D_3A) variant represents the relative population of inactive and active conformers.

As described previously by Wells,[15] the K_M of the procaspase 3 zymogen for the peptide substrate is similar to that of the mature enzyme, ~12 μM, suggesting that the contaminating cleaved product of the zymogen is the solely active form in the sample. We also observe that the K_M values of the uncleavable procaspase 3 and of the IL variants are similar to the cleaved, mature caspase 3, but we also show that the full-length protein is enzymatically active. Overall, our data suggest that the active sites of the zymogen are mostly intact and are capable of binding substrate similarly to the wild-type, cleaved, protein, while the catalytic Cys163 and His121 residues are not positioned for proper catalysis. We note that this interpretation is inconsistent with the structural data for procaspase 7 (refs 16,17), which show that the substrate-binding loop (L3) is exposed to solvent (see Figure 1C, active site 2). For procaspase 3, an exposed L3 would result in Trp206 being completely exposed to solvent in the inactive conformer while moving to a buried position in the active conformer, where the tryptophan stacks on Trp214. The projected movement of this tryptophan is inconsistent with the blue-shifted fluorescence emission profile observed for the native protein, where the tryptophans are observed in a less solvent-exposed environment in the native protein and are exposed to solvent upon unfolding.[23,33−36] Furthermore, the catalytic cysteine is highly protected against zinc ions in the zymogen compared to the mature caspase 3 (ref 32). Collectively, our data show that, although there may be adjustments in the substrate-binding loop, L3, the switch from the inactive to active conformer of the uncleavable procaspase 3(D_3A) primarily affects positioning of the catalytic cysteine, C163, into the active configuration. Moreover, our data suggest that either the crystal structures of procaspase 7 are not good models for the conformation of procaspase 3 in solution, or the uncleavable variant, procaspase 3(D_3A), is not a good model for the wild-type procaspase 3. Our biophysical studies of the catalytically inactive procaspase 3(C163S) yield similar spectroscopic properties as those of the uncleavable procaspase 3(D_3A), so the active site loops appear to be in similar conformations.[22,34] This interpretation is consistent with other groups that have shown catalytic competency in the zymogen using active site labels that require enzyme turnover.[37]

Wells and co-workers very clearly show activity in the minor population of cleaved protein for wild-type procaspase 3, and this activity appears to be important for processing the zymogen when it is immobilized on fibrils.[15] When taken together with the data presented here, the combined results suggest that the fibrils bind the inactive conformer of procaspase 3, which is prevalent in solution. In that case, activation must then occur via cleavage of the IL and subsequent active site formation (binding-then-cleavage mechanism) rather than a redistribution of the conformational ensemble to favor the active conformer. In some ways the question of "how poor an enzyme is procaspase 3?" is an argument of semantics, but it raises an important point in considering how one might target the zymogen in cancer cells. The direct activation of procaspase 3 may represent a novel method for the treatment of cancer for several reasons. We have shown that a constitutively active procaspase 3 is resistant to inhibition by endogenous apoptotic inhibitors, such as XIAP,[10] which are often overexpressed in cancer cells. Because the activation of caspase 3 is the commitment step for apoptosis, this strategy would likely be useful for the treatment of numerous cancer cell types while avoiding reduced efficacy due to drug resistance. So, how does one target procaspase 3 for activation? Wells and co-workers elegantly demonstrate that formation of fibrils either with small drug compounds or natural proteins[38] result in activation of the zymogen through a binding-then-cleavage mechanism.[15] Our data suggest that one can directly target the procaspase 3 conformational ensemble to stabilize the active conformer, possibly using small drug compounds.[13] Unfortunately, no small drug compounds have been found thus far that result in an efficient shift to the active conformer. The conformational free energy required to shift from the inactive to active conformer appears to be greater than the binding free energy for putative activators, so the reaction has been inefficient thus far. Indeed, there have been no natural activators identified *in vivo* that bind to the procaspase and shift the conformation to the active state, aside from cleavage by initiator caspases. In contrast, several mechanisms exist in cells to inactivate the protein, either through post-translational modifications of caspase 3 (refs 39−41) or by sequestering the procaspase from the initiator caspases.[42−44] In this regard, it may be necessary to explore compounds that promote the binding-then-cleavage mechanism of activation rather than compounds that promote a shift in the conformational ensemble if the binding free energy for small drug compounds is insufficient to stabilize the active conformer. A clearer picture of the conformational ensemble in the zymogen will be helpful in designing compounds directed at the active conformer. The data presented here show that such compounds will have to promote the expulsion of the IL from the interface as well as stabilize the loop bundle in the active conformation.

■ ASSOCIATED CONTENT

Supporting Information

Primers and plasmid templates used for generating procaspase 3 mutants and additional distance calculations from molecular dynamics simulations are presented. This material is available free of charge via the Internet at http://pubs.acs.org.

■ AUTHOR INFORMATION

Corresponding Author

*E-mail: clay_clark@ncsu.edu. Phone: (919) 515-5805. Fax: (919) 515-2047.

Present Address

Current Address: Joshua L. Schipper, Institute for Genome Sciences and Policy, Duke University, Durham, North Carolina 27708, United States.

Funding

This work was supported by a grant from the NIH (National Institutes of Health) [grant number GM065970 (to A.C.C.)].

Notes

The authors declare no competing financial interest.

■ ACKNOWLEDGMENTS

We thank the research agencies of North Carolina State University and the North Carolina Agricultural Research Service.

■ ABBREVIATIONS

IL, intersubunit linker; DI, dimer interface; procaspase 3(D_3A), procaspase 3 (D9A,D28A,D175A); Ac-DEVD-afc, N-acetyl-asp-glu-val-asp 7-amido-4-trifluoromethylcoumarin; Ac-DEVD-cmk, N-acetyl-L-α-aspartyl-L-α-glutamyl-N-[(1S)-1-(carboxymethyl)-3-chloro-2-oxopropyl]-L-valinamide; Z-VAD-fmk, carbobenzoxy-valyl-alanyl-aspartyl-[O-methyl]-fluoromethylketone

■ REFERENCES

(1) Favaloro, B., Allocati, N., Graziano, V., Di Ilio, C., and De Laurenzi, V. (2012) Role of apoptosis in disease. *Aging 4*, 330−349.
(2) Pop, C., and Salvesen, G. S. (2009) Human caspases: Activation, specificity, and regulation. *J. Biol. Chem. 33*, 21777−21781.
(3) Muzio, M., Stockwell, B. R., Stennicke, H., Salvesen, G. S., and Dixit, V. M. (1998) An induced proximity model for capase-8 activation. *J. Biol. Chem. 273*, 2926−2930.
(4) MacKenzie, S. H., and Clark, A. C. (2008) Targeting cell death in tumors by activating caspases. *Current Cancer Drug Targets 8*, 98−109.
(5) MacKenzie, S. H., and Clark, A. C. (2012) Death by caspase dimerization. *Adv. Exp. Med. Biol. 747*, 55−73.
(6) Stennicke, H. R., and Salvesen, G. S. (1998) Properties of the caspases. *Biochim. Biophys. Acta 1387*, 17−31.
(7) MacKenzie, S. H., Schipper, J. L., and Clark, A. C. (2010) The potential for caspases in drug discovery. *Curr. Opin. Drug Discovery Dev. 13*, 568−576.
(8) Ouyang, L., Shi, Z., Zhao, S., Want, F.-T., Zhou, T.-T., Liu, B., and Bao, J.-K. (2012) Programmed cell death pathways in cancer: a review of apoptosis, autophagy and programmed necrosis. *Cell Proliferation 45*, 487−498.
(9) Jia, L.-T., Chen, S.-Y., and Yang, A.-G. (2012) Cancer gene therapy targeting cellular apoptosis machinery. *Cancer Treat. Rev. 38*, 868−876.
(10) Walters, J., Pop, C., Scott, F. L., Drag, M., Swartz, P., Mattos, C., Salvesen, G. S., and Clark, A. C. (2009) A consitutively active and uninhibitable caspase-3 zymogen efficiently induces apoptosis. *Biochem. J. 424*, 335−345.
(11) West, D. C., Qin, Y., Peterson, Q. P., Thomas, D. L., Palchaudhuri, R., Morrison, K. C., Lucas, P. W., Palmer, A. E., Fan, T. M., and Hergenrother, P. J. (2012) Differential effects of procaspase-3 activating compounds in the induction of cancer cell death. *Mol. Pharmaceutics 9*, 1425−1434.
(12) Wolan, D. W., Zorn, J. A., Gray, D. C., and Wells, J. A. (2009) Small-molecule activators of a proenzyme. *Science 326*, 853−858.
(13) Schipper, J. L., MacKenzie, S. H., Sharma, A., and Clark, A. C. (2011) A bifunctional allosteric site in the dimer interface of procaspase-3. *Biophys. Chem. 159*, 100−109.
(14) Denault, J.-B., Drag, M., Salvesen, G. S., Alves, J., Heidt, A. B., Deveraux, Q., and Harris, J. L. (2007) Small molecules not direct activators of caspases. *Nat. Chem. Biol. 3*, 519.
(15) Zorn, J. A., Wolan, D. W., Agard, N. J., and Wells, J. A. (2012) Fibrils colocalize caspase-3 with procaspase-3 to foster maturation. *J. Biol. Chem. 287*, 33781−33795.
(16) Chai, J., Wu, Q., Shiozaki, E., Srinivasula, S. M., Alnemri, E. S., and Shi, Y. (2001) Crystal structure of a procaspase-7 zymogen: Mechanisms of activation and substrate binding. *Cell 107*, 399−407.
(17) Riedl, S. J., Fuentes-Prior, P., Renatus, M., Kairies, N., Krapp, S., Huber, R., Salvesen, G. S., and Bode, W. (2001) Structural basis for the activation of human procaspase-7. *Proc. Natl. Acad. Sci. U.S.A. 98*, 14790−14795.
(18) Boucher, D., Blais, V., Drag, M., and Denault, J.-B. (2011) Molecular determinants involved in activation of caspase 7. *Biosci. Rep. 31*, 283−294.
(19) Feeney, B., Pop, C., Swartz, P., Mattos, C., and Clark, A. C. (2006) Role of loop bundle hydrogen bonds in the maturation and activity of (pro)caspase-3. *Biochemistry 45*, 13249−13263.
(20) Witkowski, W. A., and Hardy, J. A. (2009) L2′ loop is critical for caspase-7 active site formation. *Protein Sci. 18*, 1459−1468.
(21) Datta, D., Scheer, J. M., Romanowski, M. J., and Wells, J. A. (2008) An allosteric circuit in caspase-1. *J. Mol. Biol. 381*, 1157−1167.
(22) Bose, K., Pop, C., Feeney, B., and Clark, A. C. (2003) An uncleavable procaspase-3 mutant has a lower catalytic efficiency but an active site similar to that of mature caspase-3. *Biochemistry 42*, 12298−12310.
(23) Pop, C., Chen, Y.-R., Smith, B., Bose, K., Bobay, B., Tripathy, A., Franzen, S., and Clark, A. C. (2001) Removal of the pro-domain does not affect the conformation of the procaspase-3 dimer. *Biochemistry 40*, 14224−14235.
(24) Feeney, B., Pop, C., Tripathy, A., and Clark, A. C. (2004) Ionic interactions near loop L4 are important for maintaining the active site environment and the dimer stability of (pro)caspase-3. *Biochem. J. 384*, 515−525.
(25) Wilm, M., Schevchenko, A., Houthaeve, T., Brett, S., Schweigerer, L., Fotsis, T., and Mann, M. (1996) Femtomole sequencing of proteins from polyacrylamide gels by nano-electrospray mass spectrometry. *Nature 379*, 466−469.
(26) Arnold, K., Bordoli, L., Kopp, J., and Schwede, T. (2006) The SWISS-MODEL Workspace: A web-based environment for protein structure homology modelling. *Bioinformatics 22*, 195−201.
(27) Kiefer, F., Arnold, K., Kunzli, M., Bordoli, L., and Schwede, T. (2009) The SWISS-MODEL repository and associated resources. *Nucleic Acids Res. 37*, D387−D392.
(28) Walters, J., Schipper, J. L., Swartz, P., Mattos, C., and Clark, A. C. (2012) Allosteric modulation of caspase-3 through mutagenesis. *Biosci. Rep. 32*, 401−411.
(29) Hess, B., Kutzner, C., van der Spoel, D., and Lindahl, E. (2008) GROMACS 4: Algorithms for highly efficient, load-balanced, and scalable molecular simulation. *J. Chem. Theory Comput. 4*, 435−447.
(30) Wang, J., Cieplak, P., and Kollman, P. A. (2000) How well does a restrained electrostatic potential (RESP) model perform in calculating conformational energies of organic and biological molecules? *J. Comput. Chem. 21*, 1049−1074.
(31) Jorgensen, W. L., Chandrasekhar, J., Madura, J. D., Impey, R. W., and Klein, M. L. (1983) Comparison of simple potential functions for simulating liquid water. *J. Chem. Phys. 79*, 926−935.
(32) Feeney, B., and Clark, A. C. (2005) Reassembly of active caspase-3 is facilitated by the propeptide. *J. Biol. Chem. 280*, 39772−39785.
(33) Pop, C., Feeney, B., Tripathy, A., and Clark, A. C. (2003) Mutations in the procaspase-3 dimer interface affect the activity of the zymogen. *Biochemistry 42*, 12311−12320.
(34) Bose, K., and Clark, A. C. (2001) Dimeric procaspase-3 unfolds via a four-state equilibrium process. *Biochemistry 40*, 14236−14242.
(35) Milam, S. L., and Clark, A. C. (2009) Folding and assembly kinetics of procaspase-3. *Protein Sci. 18*, 2500−2517.
(36) MacKenzie, S. H., and Clark, A. C. (2013) Slow folding and assembly of a procaspase-3 interface variant. *Biochemistry,*.
(37) Roy, S., Bayly, C. I., Gareau, Y., Houtzager, V. M., Kargman, S., Keen, S. L. C., Rowland, K., Seiden, I. M., Thornberry, N. A., and Nicholson, D. W. (2001) Maintenance of caspase-3 proenzyme dormancy by an intrinsic "safety catch" regulatory tripeptide. *Proc. Natl. Acad. Sci. U.S.A. 98*, 6132−6137.
(38) Zorn, J., Wille, H., Wolan, D. W., and Wells, J. A. (2011) Self-assembling small molecules form nanofibrils that bind procaspase-3 to promote activation. *J. Am. Chem. Soc. 133*, 10630−19633.
(39) Voss, O. H., Kim, S., Wewers, M. D., and Doseff, A. I. (2005) Regulation of monocyte apoptosis by the protein kinase Cδ-dependent phosphorylation of caspase-3. *J. Biol. Chem. 280*, 17371−17379.
(40) Eckelman, B. P., Salvesen, G. S., and Scott, F. L. (2006) Human inhibitor of apoptosis proteins: why XIAP is the black sheep of the family. *EMBO Rep. 7*, 988−994.
(41) Choi, Y. E., Butterworth, M., Malladi, S., Duckett, C. S., and Cohen, G. M. (2009) The E3 ubiquitin ligase cIAP1 binds and

ubiquitinates caspase-3 and -7 via unique mechanisms at distinct steps in their processing. *J. Biol. Chem. 284*, 12772−12782.
(42) Voss, O. H., Batra, S., Kolattukudy, S. J., Gonzalez-Mejia, M. E., Smith, J. B., and Doseff, A. I. (2007) Binding of caspase-3 prodomain to heat shock protien 27 regulates monocyte apoptosis by inhibiting caspase-3 proteolytic activation. *J. Biol. Chem. 282*, 25088−25099.
(43) Denault, J.-B., and Salvesen, G. S. (2003) Human caspase-7 activity and regulation by its N-terminal peptide. *J. Biol. Chem. 278*, 34042−34050.
(44) Van Raam, B. J., and Salvesen, G. S. (2012) Proliferative versus apoptotic functions of caspase-8. Hetero or homo: The caspase-8 dimer controls cell fat. *Biochim. Biophys. Acta 1824*, 113−122.